

Experimental evaluation of two simple thermal models using transient temperature analysis

Michael C Kolios†§, Arthur E Worthington†, Michael D Sherar‡ and John W Hunt†

† Division of Experimental Therapeutics, The Ontario Cancer Institute and Department of Medical Biophysics, University of Toronto, 610 University Avenue, Toronto, Ontario M5G-29, Canada

‡ Division of Medical Physics, The Ontario Cancer Institute and Department of Medical Biophysics, University of Toronto, 610 University Avenue, Toronto, Ontario M5G-29, Canada

Received 24 April 1997, in final form 6 July 1998

Abstract. Thermal models are used to predict temperature distributions of heated tissues during thermal therapies. Recent interest in short duration high temperature therapeutic procedures necessitates the accurate modelling of transient temperature profiles in heated tissues. Blood flow plays an important role in tissue heat transfer and the resultant temperature distribution. This work examines the transient predictions of two simple mathematical models of heat transfer by blood flow (the bioheat transfer equation model and the effective thermal conductivity equation model) and compares their predictions to measured transient temperature data. Large differences between the two models are predicted in the tissue temperature distribution as a function of blood flow for a short heat pulse. In the experiments a hot water needle, $\sim 30^\circ\text{C}$ above ambient, delivered a 20 s heating pulse to an excised fixed porcine kidney that was used as a flow model. Temperature profiles of a thermocouple that primarily traversed the kidney cortex were examined. Kidney locations with large vessels were avoided in the temperature profile analysis by examination of the vessel geometry using high resolution computed tomography angiography and the detection of the characteristic large vessel localized cooling or heating patterns in steady-state temperature profiles. It was found that for regions without large vessels, predictions of the Pennes bioheat transfer equation were in much better agreement with the experimental data when compared to predictions of the scalar effective thermal conductivity equation model. For example, at a location $r \sim 2$ mm away from the source, the measured delay time was 10.6 ± 0.5 s compared to predictions of 9.4 s and 5.4 s of the BHTE and ETCE models, respectively. However, for the majority of measured locations, localized cooling and heating effects were detected close to large vessels when the kidney was perfused. Finally, it is shown that increasing flow in regions without large vessels minimally perturbs temperature profiles for short exposure times; regions with large vessels still have a significant effect.

1. Introduction

Thermal therapies rely on increasing or decreasing tissue temperatures to cytotoxic levels to achieve a therapeutic effect. Conventional hyperthermia (target temperatures of $41\text{--}45^\circ\text{C}$), in conjunction with radiation, has demonstrated increased effectiveness in the treatment of certain types of cancer (Overgaard *et al* 1996, Vernon *et al* 1996, Valdagni and Amichetti

§ Now at: Department of Mathematics, Physics and Computer Science, Ryerson Polytechnic University, 350 Victoria Street, Toronto, Ontario M5B 2K3, Canada

1994). It is difficult to achieve and maintain the target volume to uniformly high steady-state temperatures, in part due to the inadequate heating technologies and in part due to dynamic mechanisms of heat removal by the body. This has prompted the development of technologies to deliver short intense pulses of heat (ranging from a few seconds to tens of minutes) to induce immediate tissue destruction by means of ultrasonic (Hynynen 1996, ter Haar 1995), microwave (Haines and Nath 1995) or laser (Malone and Wyman 1992) heating techniques. Interest in short duration high temperature treatments has increased due to recent developments in imaging technology that may allow near real time damage assessment and feedback control (Hynynen *et al* 1995, Cline *et al* 1993). Furthermore, temperature maps of the treatment volume may be obtainable (Vitkin *et al* 1997, Macfall *et al* 1996, Cline *et al* 1996).

The determinants of temperature distributions during thermal therapy are: the power deposition pattern of the heating source, heat removal by conduction and heat removal by blood flow forced convection (other terms, such as metabolic heat generation are small and ignored). To model the induced transient temperature distributions, additional terms are included in the heat conduction equation to take into account the effects of the heating source and of blood flow. To include the effects of blood flow, the fully conjugated tissue/blood heat transfer equations should be solved for all vessels in the region of interest (Huang *et al* 1996). However, due to the large number of vessels and their complex geometry, the equations are difficult to solve. Therefore, to approximate the effects of blood flow through the numerous smaller vessels of the circulation, macroscopic models are used that average the effects of many vessels. Hence, two terms are added to the heat conduction equation to take into account blood flow: one term that models individual large vessels (an advective term to model convective heat transfer by the moving blood) and one term that models the effects of smaller vessels that cannot induce significant localized temperature gradients (Legendijk 1990). Large vessels that induce localized gradients are also termed thermally significant vessels and the extent of the temperature gradients depend mainly on the vessel diameter and the volumetric blood flow rate through the vessel (Chato 1980). Theoretical work has shown that vessels with diameters larger than ~ 0.5 mm belong to this category (Roemer 1991, Crezee 1993, Kolios *et al* 1996).

Several models have been proposed to quantify the collective effect of thermally insignificant vessels. The two simplest and most utilized models for hyperthermia treatment planning are the Pennes bioheat transfer equation (BHTE) and the effective thermal conductivity equation (ETCE). In the BHTE model heat transfer between the blood vessels and tissue is assumed to occur mainly across the capillaries where blood velocity is low (Pennes 1948). The blood in the capillary bed instantly thermally equilibrates with the temperature of the surrounding tissue and enters the venous circulation at the local tissue temperature. Therefore, the contribution of blood flow could be modelled as a heat sink whose magnitude is proportional to the difference between the arterial supply temperature and the local tissue temperature. In the ETCE model it is assumed that blood thermally equilibrates before reaching the capillary level. The mean tissue temperature is determined by countercurrent pairs of closely spaced and nearly equilibrated vessels (Weinbaum *et al* 1984). Provided that the majority of heat is conducted between the countercurrent vessels, heat transfer due to such vessel pairs can be accounted for by using an effective conductivity tensor in the heat conduction equation. Under certain conditions, the tensor could simplify to a scalar. A critical review of these and other thermal models can be found in Arkin *et al* (1994).

The goal of this work is to determine which microvascular heat transfer model (the BHTE or the ETCE) is more accurate in predicting temperature profiles of tissues during

transient heating. Both the ETCE model (Wyman and Whelan 1994, Whelan and Wyman 1995, Loyd *et al* 1997) and the BHTE model (Martin *et al* 1992, Kolios *et al* 1996, Shaw *et al* 1996) have been used to predict temperature distributions. Furthermore, treatment strategies have been proposed and designed based on these results. Since predictions of the two models diverge as tissue blood flow increases (section 2), it is important to determine which model offers a more accurate description of the temperature distributions during tissue heating in the absence of large vessels.

In the few other published comparisons of transient temperature predictions of the BHTE and ETCE with experimental data for tissue heating, Crezee (1993) concluded that the ETCE is more accurate by examining the time–temperature profiles after a step-wise change in the heating source for a fixed bovine kidney (Crezee and Lagendijk 1990) and a freshly excised bovine tongue (Crezee *et al* 1991). They demonstrated a decrease in the delay time (the time delay between the initial temperature rise of the source and the temperature rise at some point r away from the source) as a function of flow, in accordance with predictions of the ETCE. Other investigators have examined steady-state temperature distributions. Moros *et al* (1993) and Rawnsley *et al* (1994) concluded that the BHTE is a better model based on profiles obtained during the ultrasonic heating of the dog thigh. In other experiments (Valvano *et al* 1994, Zhu *et al* 1994, Crezee 1993), the ETCE was found to be a better approximation. In the above experiments however either the effects of large vessels were not excluded (which complicates the analysis), the spatial temperature sampling was relatively sparse or the analysis was performed in small regions. Furthermore, temperature profiles over large tissue regions as a function of time have not been examined. Such profiles are sensitive to the differences in the model predictions of the BHTE and ETCE.

In our work, we compare the predictions of the two simplified thermal models to experimental transient temperature profiles measured in a fixed porcine kidney attached to a perfusion circuit. By controlling kidney inflow and measuring the tissue transient temperature response to a 20 s heat pulse, we compare the results to theoretical predictions. Since thermally significant vessels have the capacity to transport heat (thus in certain cases emulate an increase in tissue conductivity in regions surrounding the vessels), analysis of temperature profiles in regions close to thermally significant vessels was avoided. The temperature profiles were analysed by examining transient temperature profiles at selected locations or by constructing spatial temperature maps at various timepoints and comparing them to theoretical predictions.

2. Theory

We consider the transient tissue response to a pulse of heat as a function of microvascular flow in the absence of thermally significant vessels. The cylindrical geometry used to calculate the transient temperature distributions resulting from a cylindrical conduit that carries hot water is shown in figure 1. The following equations were solved computationally by the method of finite differences:

$$\rho_f c_f \frac{\partial T}{\partial t} = k_f \left(\frac{\partial^2 T}{\partial^2 r} + \frac{1}{r} \frac{\partial T}{\partial r} + \frac{\partial^2 T}{\partial^2 z} \right) - \rho_f c_f u(r) \frac{\partial T}{\partial z} \quad (1)$$

$$\rho_t c_t \frac{\partial T}{\partial t} = k_{\text{eff}} \left(\frac{\partial^2 T}{\partial^2 r} + \frac{1}{r} \frac{\partial T}{\partial r} + \frac{\partial^2 T}{\partial^2 z} \right) - w_b c_b (T(r, z) - T_{\text{art}}) \quad (2)$$

where ρ is the density (g cm^{-3}), c is the specific heat capacity ($\text{J g}^{-1} \text{ }^\circ\text{C}^{-1}$), T is the temperature ($^\circ\text{C}$), $u(r)$ is the velocity of blood (cm s^{-1}), k is the thermal conductivity

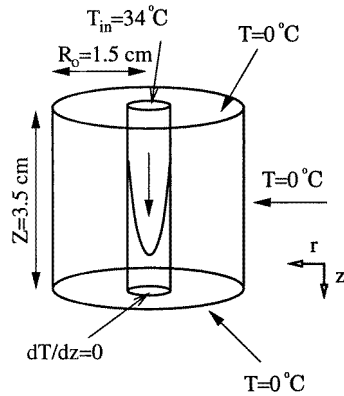


Figure 1. The geometry and boundary conditions used in the theoretical model. The temperatures represent temperature above ambient.

($\text{W cm}^{-1} \text{ } ^\circ\text{C}^{-1}$), w is the volumetric perfusion rate ($\text{g cm}^{-3} \text{ s}^{-1}$) and k_{eff} is the tissue effective conductivity for the ETCE. Subscripts *art*, *b*, *f* and *t* denote arterial, blood, fluid and tissue respectively. Equation (1) models the hot water heat source while equation (2) models heat transfer in tissue.

The thermal parameters used in the simulations are listed in table 1. The radial and axial boundary conditions were chosen to match the geometry of the kidney and the experimental conditions. The outer radius R_o was set to 1.4 cm and the cylinder length L to 3.5 cm to match the dimensions of the kidney slice in the plane of three of the thermocouple paths (see section 3.1). The radial boundaries were set to the ambient temperature, T_0 . The axial boundaries were set as follows: at $z = 0$ and within the fluid domain the temperature was set to the input fluid temperature T_{in} while in the tissue domain it was set to T_0 . Thus, the inner cylindrical vessel was the heat source. In all simulations the arterial temperature was equal to T_0 . The thermal pulse duration was set to 20 s to match the pulse duration in the experimental studies. The velocity profile $u(r)$ in equation (1) was chosen to be parabolic since the fluid was fully developed. At $z = L$ within the fluid domain an adiabatic boundary condition was implemented while in the tissue domain the temperature was set to T_0 . The grid spacing in the axial direction dz was set to 0.1 mm while in the radial direction the grid spacing dr varied linearly from 0.0001 mm at the centre to 0.2 mm. The timestep dt was set to 0.1 s. Further details on the computational method can be found elsewhere (Kolios *et al* 1994, 1995). In this formulation, no prior assumptions are made with respect to heat transfer coefficients at the radial boundary of the cylinder and tissue. This is expected to produce more accurate results than if heat transfer coefficients are used (Kolios *et al* 1995).

Table 1. Listing of physical parameters used in simulations (Duck 1990).

Tissue specific heat capacity, c_t ($\text{J g}^{-1} \text{ } ^\circ\text{C}^{-1}$):	4.180
Tissue density, ρ_t (g cm^{-3}):	1.000
Tissue conductivity, k_t ($\text{W cm}^{-1} \text{ } ^\circ\text{C}^{-1}$):	0.006
Blood and fluid specific heat capacity, c_b ($\text{J g}^{-1} \text{ } ^\circ\text{C}^{-1}$):	4.180
Blood and fluid density, ρ_f (g cm^{-3}):	1.000
Perfusion rate, w_b ($\text{g cm}^{-3} \text{ s}^{-1}$):	variable
Fluid average velocity, u_{avg} (cm s^{-1}):	45

The BHTE was modelled by setting $k_{\text{eff}} = k_t$ in equation (2) and adjusting w_b to the perfusion value of the tissue examined. Similarly, for the ETCE model, w_b was set to zero and k_{eff} assigned the value of interest. To directly compare the results, volumetric perfusion and effective conductivity were related according to the experimental data of Crezee and Legendijk (1990):

$$k_{\text{eff}} = k_t(1 + \beta w_b) \quad (3)$$

where $\beta = 0.12 \text{ (ml/100 g min}^{-1}\text{)}^{-1}$. Perfusion values were converted from ml/100 g min^{-1} to $\text{g cm}^{-3} \text{ s}^{-1}$ by assuming a tissue density of 1 g cm^{-3} . To compare the theoretical and experimental results, kidney perfusion was estimated by taking the ratio of the renal artery inflow and the kidney mass. Perfusion was assumed uniform throughout the entire tissue volume.

Predictions of the two models diverge for increasing blood flow. Changes in the tissue effective conductivity as a function of blood flow in the ETCE (equation (3)) result in an increase in tissue effective diffusivity α_{eff} since $\alpha = k_{\text{eff}}/\rho_t c_t$. The increase in tissue effective diffusivity and conductivity results in accelerated tissue heat transfer and smoothes the sharp temperature gradients created by the heating source. In contrast, tissue conductivity and diffusivity remains unaltered in the BHTE. Therefore, predictions of the BHTE indicate that microvascular flow has small effects on the temperature distribution for short heating times and temperature profiles retain the original shape of the heating source for a longer period of time.

3. Methods

3.1. Experimental methods

An 80 g fixed porcine kidney was used as a perfusion model according to the protocol developed by Holmes *et al* (1984) and modified by Jia (1995). In this procedure the organ is fixed such that the vasculature retains its integrity allowing it to be used as a flow phantom when perfused *ex vivo*. X-ray images using water-soluble iodine contrast agents and temperature pulse-decay experiments confirmed that mass and thermal clearance mechanisms of the kidney were not compromised by the fixation (Jia 1995). However, insertion of probes and repeated experiments did result in an increase in kidney vascular resistance over time.

The kidney was perfused with distilled de-ionized water controlled by a computerized peristaltic pump (Masterflex, model 7550-600, Barrington, IL, USA) connected to a pressure meter (DRUCK GLA Electronica 86-20, Milan, Italy), bubble trap and filter (Milipore Corporation, Bedford, MA, USA) (figure 2). Kidney perfusate was circulated through a heat exchanger located in the waterbath to ensure that the perfusate and waterbath temperatures were equal. Inflow pressure was limited to a maximum of 125 mm Hg to avoid vascular damage. Circuit pressure differential was achieved by using a water reservoir elevated 1.85 m above the kidney level as indicated in figure 2.

The kidney was immersed in a waterbath at room temperature. The waterbath was stirred by connecting it to a circulation circuit (flow rate $\simeq 4 \text{ l min}^{-1}$) and a thermocouple was used to measure the waterbath temperature. The heat source consisted of an 18 gauge (1.2 mm outer diameter) needle perfused with hot (40–60 °C) water to induce temperature gradients in the tissue. The temperature of the water was monitored at the entry and exit of the needle. Needle flow was achieved by use of the water reservoir discussed previously (volumetric flow through needle $\simeq 1.2 \text{ ml s}^{-1}$). A computer controlled pinch valve (Cole

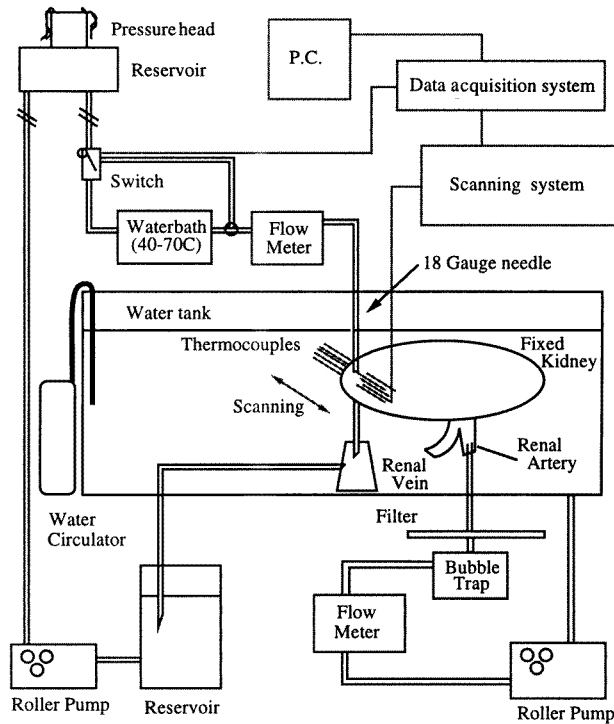


Figure 2. The experimental system built to determine the differences in the transient temperature profiles near a heat source as a function of perfusion. It consists of four main components: two flow circuits (for the kidney and the heat source), a scanning system and a thermometry data acquisition system. Five thermocouples are scanned in steps of 100 μm , providing high spatial resolution measurements.

Parmer, part H-98301-22, Chicago, IL, USA) was used to switch between hot ($\sim 60^\circ\text{C}$) and room temperature water to deliver a 20 s heat pulse to the kidney. The experimental protocol is shown schematically in figure 3(a). Thermocouples were placed at the needle inlet and outlet to record the pulse temperature for each experiment.

Five type K chromel–alumel thermocouples, each of 50 μm diameter and forming a junction approximately 0.1–0.2 mm in diameter, were encased in fused silica tubes of 0.5 mm outer diameter. The tubes were glued to the kidney surface using a commercial adhesive (cyanoacrylate ester, Loctite Corp.). A multifunction 16 channel data acquisition system (Labmate Scienmetrics, Nepean, Ontario, Canada) recorded the thermocouple measurements which were stored on a personal computer and later analysed. The thermocouples were calibrated in a waterbath against a standard mercury thermometer (Fisher, Canada) and had an accuracy of $\pm 0.1^\circ\text{C}$. The thermocouples were scanned by attaching them to a plastic mount that was driven by a stepping motor (rotor SLS-4014-002 model, Princeton, IN, USA) and incremented in steps of 0.1 mm ($\pm 5\%$ per step). Ambient temperature was 26°C and thus T_{in} , the difference between the inlet and ambient temperature, was $\sim 34^\circ\text{C}$. The peristaltic pump and the pinch valve were controlled by the data acquisition software. The tissue temperatures were recorded at a temporal sampling rate of 1.04 s^{-1} and sampling continued for either 120 s or 150 s after the heat pulse. To accelerate kidney cooling before stepping the thermocouples to another location the kidney inflow was set to 40 ml min^{-1} for

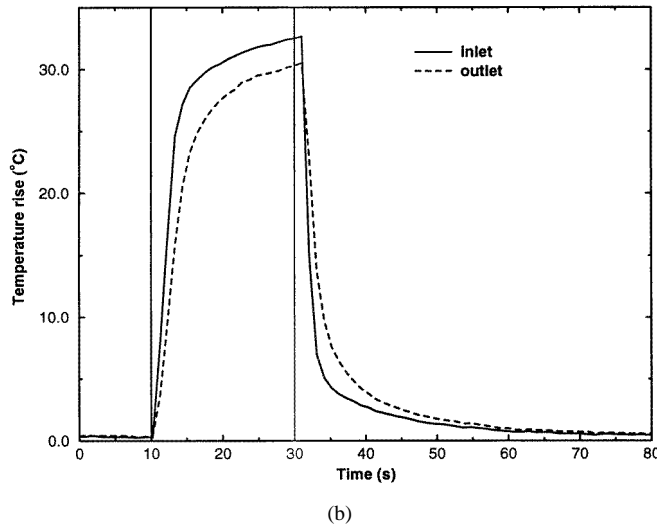
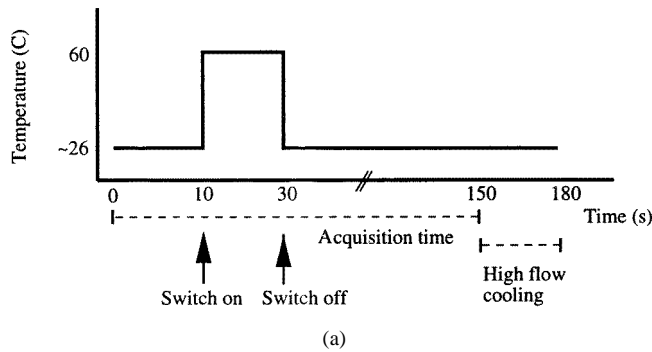


Figure 3. The heating protocol for the transient experiments. (a) A 20 s duration pulse of heated water enters the needle and temperature data are collected for 1–2 min. Data acquisition is followed by a 20–30 s ‘cooldown’ of the kidney. (b) Typical measured temperatures in the pulse heating experiments at the entrance and exit of the needle source. Vertical lines represent pulse on and off times (on and off times of the control switch).

20 s after data acquisition. Temperature data at the new location were not analysed unless the thermocouple readings were within 0.5°C of the ambient waterbath temperature before the pulse initiation. Pre-selected regions of the kidney were scanned to reduce acquisition time. Each 8 mm kidney scan (in steps of 0.1 mm) took approximately $3\frac{1}{2}$ hours to complete.

The locations of the thermocouple paths with respect to the heating source and the kidney vasculature were determined using high resolution x-ray computed tomography (CT) as described in more detail elsewhere (Kolios *et al* 1998). Briefly, after all the heat transfer experiments were completed, an iodine based nanoparticulate contrast agent (Gazelle *et al* 1994) was injected into the kidney and CT data were collected using a high resolution volumetric CT scanner (Holdsworth *et al* 1993). The distances between the thermocouple path and the heating source or large blood vessels were measured from this dataset. For the thermocouple path for which the analysis was done (section 3.2), the minimum distance between the thermocouple path and the source was ~ 1.2 mm. Locations close to large vessels were avoided in the data analysis. Since thermally significant vessels are a function of both flow and vessel size and only vessel size can be estimated from the CT data,

steady-state temperature profiles in the same kidney in which the transient experiments were performed were collected to detect thermal gradients near the vessels. Locations where thermal gradients due to vessels were detected (by comparing the steady-state profiles with and without flow) were avoided.

3.2. Data analysis

Model comparison was performed by analysis of either the transient temperature profiles at a specific location or the shape of the temperature profiles at a specific time during the experiment. The analysis was limited to the one thermocouple path (labelled L in figure 4) that did not cross large vessels according to the CT dataset. Furthermore, this thermocouple did not record the thermal signatures characteristic of large vessels in the steady-state experiments.

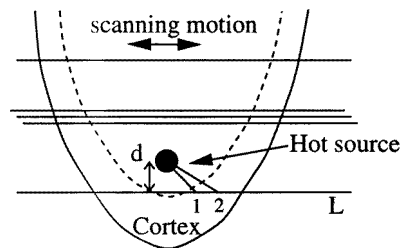


Figure 4. Highly schematic diagram of thermocouple paths in the kidney. Dotted lines represent the boundary between the kidney medulla and cortex (outer shell). Analysis was performed for the thermocouple labelled L. The distance d (minimum distance between the source and thermocouple path) was 1.2 mm. Locations 1 and 2 are a distance $r = 2$ mm and 4.2 mm away from the source, respectively.

To quantify the time–temperature profiles the delay time was used. The delay time is defined in this work as the time interval between the start of the pulse and the time at which the temperature reached 0.632 of the maximum temperature. Since the temperature may not have been sampled at this exact timepoint, a linear interpolation was used to calculate the time at which the temperature reached 0.632 of the maximum temperature. At locations where the delay time was measured, ten temperature profiles were collected and averaged. Two locations were chosen for analysis: one close to the source to minimize the effects of the kidney boundaries ($r = 2.0$ mm) and one further from the source to emphasize the difference in model predictions ($r = 4.2$ mm). To reconstruct the temperature profile at a specific time during the heating experiment temperature data at the timepoint of interest were extracted from the files that contained the temporal temperature measurements at each location scanned. For each pulse experiment the timepoint at which data was collected varied slightly; however, the extracted data from all of the sets did not deviate more than ± 0.5 s for a specific timepoint of interest. The data presented in this format represent the average of three runs.

4. Results

The temperature profiles of the heating pulse measured at the entrance and exit of the needle are shown in figure 3(b). The profiles slightly deviate from the idealized theoretical

square pulse of figure 3(a) that was used in the simulations. The 20 s pulse resulted in a transient temperature increase in the kidney tissue. Analysis of the temperature profiles was performed at kidney locations for which there was no evidence of localized temperature gradients caused by large vessels. A comparison of the theoretical predictions and the experimental data with no kidney flow (i.e. a pure conduction problem) for two such locations is shown in figure 5. Figures 5(a) and 5(c) demonstrate theoretical (dashed lines) and experimental (solid lines) data for $r = 2.0$ mm and $r = 4.2$ mm (figure 4). There is good agreement between the theoretical and experimental curves. The experimental profiles generally lag the theoretical profiles by 2–3 s and the cooling rates are underestimated for locations far from the source. The temperature data measured at the same locations for a kidney inflow of 30 ml min^{-1} are shown in figures 5(b) and 5(d). The predictions of the BHTE model are denoted with the long dashed line and the predictions of the ETCE model are denoted with the dotted–dashed line. Equation (3) was used to estimate the effective conductivity of the perfused tissue. While the ETCE model predicts a significant increase in the maximum temperature (up to three times greater at $r = 4.2$ mm) and a decrease in the delay time (up to 50% at $r = 4.2$ mm), the BHTE predicts a small decrease in the maximum temperature and delay times. The experimental data reveal small changes in the delay time with flow and a decrease in maximum temperature (figures 5(b) and 5(d)). Delay times as a function of flow are summarized in tables 2 and 3 for the corresponding locations for which the temperatures were measured in figure 5.

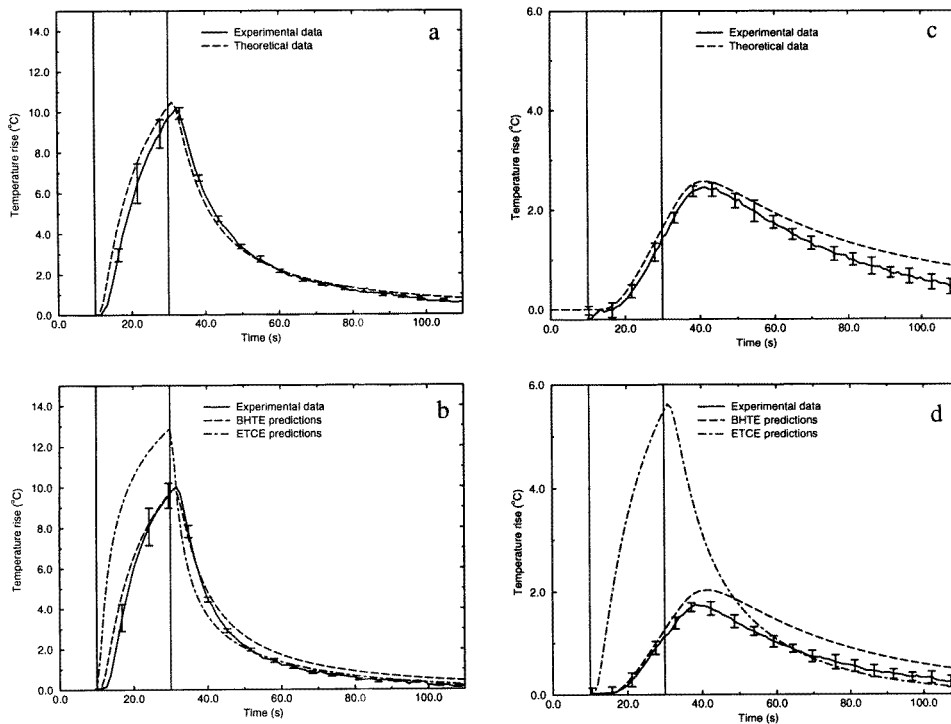


Figure 5. Comparison of theoretical and experimental data for two locations in the kidney ((a) and (b) at $r = 2$ mm and (c) and (d) at $r = 4.2$ mm). Figures (a) and (c) demonstrate the temperature data with no flow and (b) and (d) with a kidney inflow of 30 ml min^{-1} . Error bars represent \pm two standard deviations. Vertical bars represent the pulse on and off times.

Table 2. Predicted and measured delay times (± 2 standard deviations) for a location $r = \sim 2$ mm from the heat source.

Flow (ml min ⁻¹)	Delay time (s)		
	BHTE	ETCE	Experimental
0	9.7	9.5	11.5 \pm 0.4
10	9.6	6.8	10.8 \pm 0.4
20	9.5	5.8	10.7 \pm 0.4
30	9.4	5.4	10.6 \pm 0.5

Table 3. Predicted and measured delay times (± 2 standard deviations) for a location $r = \sim 4.2$ mm from the heat source.

Flow (ml min ⁻¹)	Delay time (s)		
	BHTE	ETCE	Experimental
0	20.0	20.0	21.2 \pm 0.6
10	19.7	14.0	20.9 \pm 0.7
20	19.5	11.6	N/A
30	19.3	10.5	19.6 \pm 1.2

The shapes of the temperature profiles at specific times after the pulse initiation were also compared to predictions of the thermal models. Figure 6 demonstrates the theoretical (long dashed lines) and experimental (solid lines) data collected for three different timepoints (5, 20 and 40 s after pulse initiation) during the experiments for no kidney flow. The times were chosen to represent snapshots of the temperature profiles during the heating phase (5 s), and the end of the pulse (20 s) and during tissue cooling (40 s). There is good agreement between experiment and theory for the conduction only problem. The 'dip' in the temperature profile for $t = 40$ s after the pulse is due to the cooling from the needle which is perfused with room temperature water after the hot pulse. The experimental data for a kidney flow of 30 ml min⁻¹ are shown in figure 7(a) superimposed with the predictions of the BHTE and in figure 7(b) superimposed with the predictions of the ETCE. The BHTE predicts the major characteristics of the temporal evolution of the temperature distribution while the ETCE does not.

5. Discussion

In regions without large vessels, predictions of the BHTE were in better agreement with the experimental temperature profiles measured. The ETCE predicts a significant decrease in the delay time and an increase in the maximum temperature for the locations examined (figures 5(b) and 5(d) and tables 2 and 3). The measured change in delay time as a function of flow in the experiments however is negligible and the maximum temperature decreases, in accordance with the predictions of the BHTE. The predictions of the BHTE better match not only the experimental data for the two locations chosen to perform the analysis (tables 2 and 3 and figures 5(b) and 5(d)) but also in terms of the temporal evolution of the spatial temperature distribution (figure 7(a)). The difference between model predictions is more evident at locations far from the source. Regions further from the source however are

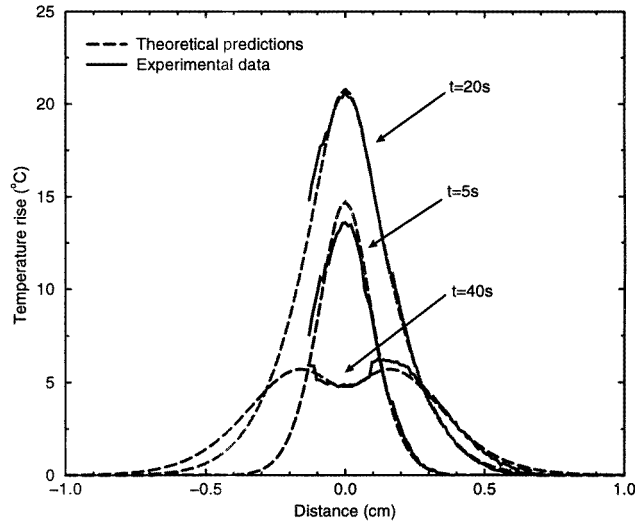


Figure 6. A comparison of theoretical (dashed curves) and experimental (8 mm segment, solid curves) temperature profiles for no kidney flow for three timepoints ($t = 5, 20$ and 40 s after pulse initiation).

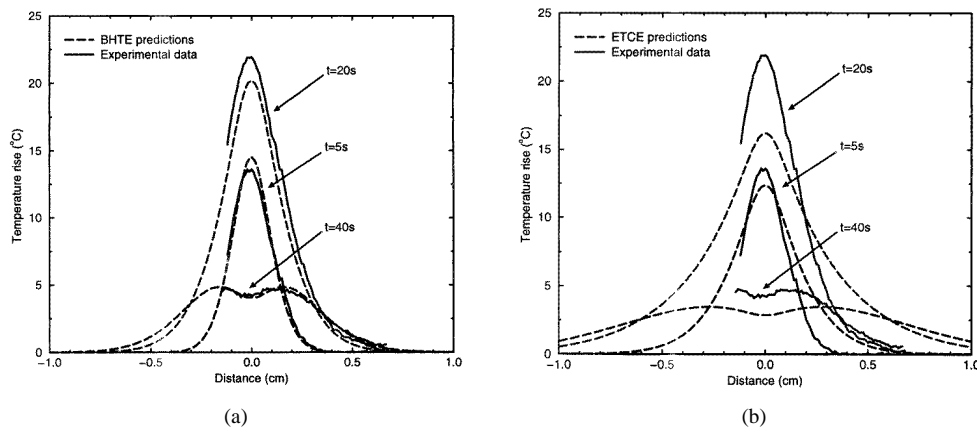


Figure 7. (a) A comparison of theoretical (BHTE model, dashed curves) and experimental (for an 8 mm segment, solid curves) temperature profiles for a kidney inflow of 30 ml min^{-1} for three timepoints ($t = 5, 20$ and 40 s after pulse initiation). (b) The same comparison using the ETCE model to calculate the theoretical curves.

also closer to the kidney boundaries for which the theoretical models are less accurate. This is the reason the two locations were chosen: one 2 mm from the source (to avoid boundary effects) and one 4.2 mm away (to maximize the model differences). Furthermore, the regions were chosen to avoid the effects of thermally significant vessels that would invalidate (or make very difficult) the comparison of the BHTE and ETCE. This was done by (a) locating and avoiding regions with spatial temperature gradients caused by thermally significant vessels in the steady state and (b) using volumetric CT angiography to estimate the proximity of large vessels to the thermocouple paths.

The experimental data indicate that an increase in microvascular perfusion does not significantly influence the temperature–time curves for short heat pulses, even though the cooling rates increase (figure 5). This is consistent with other theoretical work demonstrating that for short heating times blood flow does not substantially affect the thermal dose delivered to tissues if the BHTE is used as the microvascular heat transfer model (Billard *et al* 1990, Hunt *et al* 1991). In contrast, the ETCE predictions show that the temperature profiles during short duration heating would be sensitive to such flow variations (figures 5(b), 5(d) and 7). Similar results were obtained when using the ETCE to model temperature distributions during ultrasonic heating (Kolios *et al* 1996).

Perfusion estimates used in the theoretical calculations were derived by dividing total kidney inflow by the kidney weight and uniform perfusion was assumed throughout the region of interest. Since the kidney perfusion is higher in the cortex, this estimate is likely to underestimate kidney perfusion at the location of measurement (the majority of the thermocouple measurements were in the kidney cortex). This is consistent with the fact that the temperature decay of all of the experimental data is greater than the BHTE predictions (figures 5(b) and 5(d)). Underestimating the perfusion would produce small changes in the predictions of the BHTE since the profiles are relatively insensitive to perfusion. For example, a good fit to the experimental decay data for a kidney inflow of 30 ml min^{-1} was obtained in the simulations using the BHTE and a volumetric flow rate of 70 ml min^{-1} . When this new flow rate was used in the computational model the predicted delay time became 8.8 s and 18.7 s for the first and second measurement point, respectively. These represent small changes in the delay time (3% and 2% with respect to the delay times calculated using a simulation flow of 30 ml min^{-1}). Interestingly, the input value of 70 ml min^{-1} predicted a percentage change in the delay time between no flow and the highest flow that fits the experimental data better for both locations. For example, at the first location the measured change in the delay time is 8% (table 2) while the predicted changes are 3% and 9% for simulation flows of 30 and 70 ml min^{-1} respectively.

Deviations in the predicted and measured temperature profiles for the unperfused kidney are shown in figures 5(a), 5(c) and 6. These are due to several factors. Small errors in the estimated thermocouple location, due to the sharp thermal gradients created by the source (as high as $5\text{--}6^\circ\text{C mm}^{-1}$), can give rise to substantial errors in the absolute temperature and the heating and cooling rates. Moreover, artifacts caused by x-ray reflection near the source contribute to errors in the calculation of the distance between the source and the thermocouple paths. Furthermore, the shape of the pulse in figure 3(b) deviates from the ideal square pulse of heat used in the theoretical calculations and may contribute to the difference in the predicted and measured delay times. This is consistent with the observation that all the experimental profiles lag their theoretical counterparts in the early portion of the heating curves (figure 5). Other limitations include the modelling of the kidney as a homogeneous cylindrical volume of tissue and the omission of the physical properties of the steel needle in the theoretical model (section 2). However, despite all of the above limitations, there is reasonable agreement between experiment and theory (figures 5(a), 5(c) and 6). This demonstrates that the above limitations do not significantly affect the results, in part because transient profiles are less sensitive to the boundary conditions of the system.

It has been shown that some of the original underlying assumptions in the derivation of the Pennes bioheat transfer equation are incorrect (Chen and Holmes 1980, Weinbaum *et al* 1984). Furthermore, recent theoretical work (Brinck and Werner 1994a, b, Huang *et al* 1996, Weinbaum *et al* 1997) suggests that the perfusion term w_b in the Pennes formulation of the bioheat transfer equation is not the ‘true’ tissue perfusion as calculated by the mass

flow rate. Brinck and Werner (1994a) suggest that the perfusion rate should be multiplied by an efficiency function that depends on the local vasculature and blood flow rate. In the Weinbaum *et al* (1997) formulation, the equivalent 'efficiency' function (termed correction coefficient) depends only on the local vascular and tissue geometry. Both approaches try to account for the heat transfer that occurs along the branching countercurrent vessel networks of skeletal muscle. Provided that these corrections also applied to the pig kidney, the BHTE predictions would be modified by a scaling factor that would be a function of the local vasculature. The efficiency function for the pig kidney for either approach has not yet been calculated. In either case, these corrections would not influence the effective diffusivity of the perfused tissue since in form it is similar to the BHTE. Thus, the conclusion that the original Pennes bioheat transfer equation (or some close derivative in form) is more appropriate for the modelling of tissue transient temperature distributions still holds. This work also suggests that the use of an effective conductivity to model non-thermally-significant blood flow would lead to erroneous results, at least for the vascular architecture in the kidney cortex.

The large differences in model predictions using transient analysis of temperature profiles make it a more sensitive technique to examine the differences between the BHTE (or similar derivative equations) and the ETCE than analysis of the steady-state temperature profiles. Analysis of the steady-state temperature profiles has been used to compare model predictions, mainly based on quantitative analysis of the shape of the temperature distributions (Crezee 1993, Moros *et al* 1993, Rawnsley *et al* 1994). Profile shape at the steady state however is more sensitive to the boundary conditions and can complicate the analysis. On the other hand, in the transient analysis the tissue diffusivity is highly sensitive to changes in tissue conductivity (i.e. tissue effective conductivity due to blood flow) as seen in figure 5, and less sensitive to the boundary conditions.

It should be noted that in four of the five thermocouple paths the presence of large vessel heat transfer was detected and had a major influence on the temperature profiles. The analysis of this data is the subject of another paper (Kolios *et al* 1998). A relevant example of these effects however (for a different thermocouple path) is shown in figure 8. As kidney inflow was increased, an increase in the maximum temperature and decrease in the delay time was observed, as would be predicted by the ETCE. Analysis of the angiography data demonstrated that a large vessel that skimmed the heating source also passed close to the thermocouple path at the location the temperature was measured in figure 8. Interestingly, even though the ETCE does not model large vessel heat transfer, the theoretical data in the above figure *qualitatively* match the experimental data at the location $r \sim 1$ cm from the source. This would indicate that the vessel (or vessels) could behave as a 'line' of increased conductivity. Therefore, without prior examination to detect thermally significant vessels, erroneous conclusions can be made when evaluating bioheat transfer models. The above observation may partially explain why other groups record reductions in delay time as a function of flow in bioheat transfer experiments and thus conclude the ETCE is a more accurate model (Crezee and Lagendijk 1990).

Finally, to accurately predict temperature profiles in heated tissues with thermally significant vessels, simple models such as the BHTE and the ETCE are inadequate. Even for high temperature short pulses in the range of 5–20 s, which tend to minimize the effects of the blood flow, flow dependent perturbations due to large vessels in the temperature distributions can be detected, such as in figure 8. Therefore, future work should focus on a practical means for incorporating angiographic data and the effects of thermally significant vessels in bioheat transfer models. This is the focus of several groups including our own (Kotte *et al* 1996, Dutton 1993, Mooibroek and Langendijk 1991).

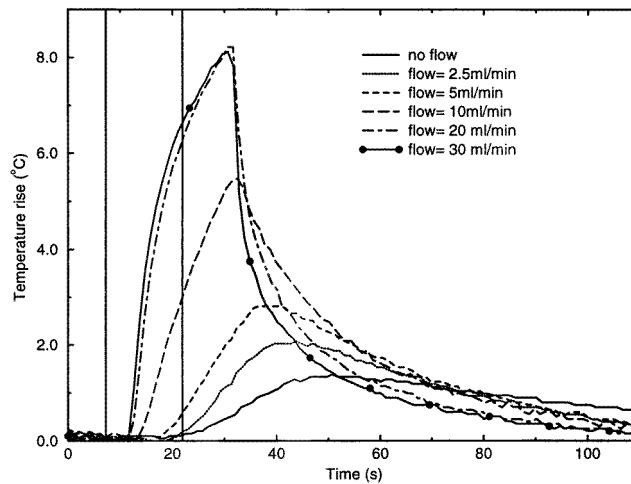


Figure 8. Temperature profiles for a thermocouple path in which a thermally significant vessel was implied by analysis of steady-state temperature distributions and angiographic data. A sharp increase in temperature rise and decrease of delay time as a function of flow is observed.

6. Conclusions

The flow dependence of transient temperature profiles in a heated fixed porcine kidney in regions without large vessels was examined. These transient studies strongly support predictions of the BHTE model of heat transfer at locations where there are no large vessels in the kidney. Transient temperature distributions are sensitive to the BHTE and ETCE model differences and should be a preferred method for their validation. Temperature profiles near large vessels that could not be modelled using these simplified models were detected in the majority of the thermocouple paths. Finally, it was shown that while an increase in perfusion has a small effect on the temperature profiles for short pulses, large vessels still have a significant effect. Future efforts in thermal modelling of rapid heating treatments should focus on the incorporation of large vessel geometry and flow data in thermal models.

Acknowledgments

The authors would like to gratefully acknowledge the financial support of the National Cancer Institute of Canada and the Ontario Cancer Treatment and Research Foundation. The first author is a recipient of a University of Toronto Open Doctoral Fellowship and an Ontario Graduate Fellowship. The authors also acknowledge the expert help of Dr David Holdsworth, Valdemar Dabrowski and Mike Thornton of the Robarts Research Institute (London, Ontario) for performing the 3D Computed Tomography studies of the kidney and Dr Gregory McIntire of Nycomed Corporation for providing the contrast agent used in the studies and his advice. Finally, the authors thank Dalton Newcombe and the Electronics Department of the Princess Margaret Hospital for their help with various aspects of this project.

References

- Arkin H, Xu L X and Holmes K R 1994 Recent developments in modeling heat transfer in blood perfused tissues *IEEE Trans. Biomed. Eng.* **41** 97–107
- Billard B E, Hynynen K and Roemer R B 1990 Effects of physical parameters on high temperature ultrasound hyperthermia *Ultrasound Med. Biol.* **16** 409–20
- Brinck H and Werner J 1994a Efficiency function: improvement of classical bioheat approach *J. Appl. Phys.* **77** 1617–22
- 1994b Estimation of the thermal effect of blood flow in a branching countercurrent network using a three-dimensional vascular model *J. Biomech. Eng.* **116** 324–30
- Chato J C 1980 Heat transfer to blood vessels *J. Biomech. Eng.* **102** 110–18
- Chen M M and Holmes K K 1980 Microvascular contributions to tissue heat transfer *Ann. NY Acad. Sci.* **335** 137–50
- Cline H E, Hynynen K, Schneider E, Hardy C J, Maier S E, Watkins R D and Jolesz F A 1996 Simultaneous magnetic-resonance phase and magnitude temperature maps in muscle *Magn. Reson. Med.* **35** 309–15
- Cline H E, Schenck J F, Watkins R D, Hynynen K and Jolesz F A 1993 Magnetic resonance-guided thermal surgery *Magn. Reson. Med.* **30** 98–106
- Crezee J 1993 Experimental verification of thermal models *PhD Thesis* University of Utrecht
- Crezee J and Lagendijk J J W 1990 Experimental verification of bio-heat transfer theories: measurement of temperature profiles around large artificial vessels in perfused tissue *Phys. Med. Biol.* **35** 905–23
- Crezee J, Mooibroek J, Bos C K and Lagendijk J J W 1991 Interstitial heating: experiments in artificially perfused bovine tongues *Phys. Med. Biol.* **36** 823–33
- Duck F A 1990 *Physical Properties of Tissues: a Comprehensive Reference Book* (San Diego, CA: Academic)
- Dutton A W 1993 A finite element solution to conjugated heat transfer in tissue using magnetic resonance angiography to measure the *in vitro* velocity field *PhD Thesis* University of Arizona
- Gazelle G S, Wolf G L, Bacon E R, McIntire G L, Cooper E R and Toner J L 1994 Nanocrystalline computed tomography contrast agents for blood-pool and liver-spleen imaging. *Invest. Radiol.* **29** (Supplement 2) S286–8
- Haines D E and Nath S 1995 New horizons in catheter ablation *J. Intervent. Cardiol.* **8** 845–56
- Holdsworth D W, Drangova M and Fenster A 1993 A high-resolution XRRI-based quantitative volume CT scanner *Med. Phys.* **20** 449–62
- Holmes K R, Ryan W, Wienstein P and Chen M M 1984 A fixation technique for organs to be used as perfused tissue phantoms in bioheat transfer studies *ASME Adv. Bioeng.* 9–10
- Huang H W, Chen Z P and Roemer R B 1996 A counter current vascular network model of heat-transfer in tissues *J. Biomech. Eng.* **118** 120–9
- Hunt J W, Lalonde R J, Ginsberg H, Urchuck S and Worthington A 1991 Rapid heating: critical theoretical assessments of thermal gradients found in hyperthermia treatments *Int. J. Hyperth.* **7** 703–18
- Hynynen K 1996 Focused ultrasound surgery guided by MRI *Sci. Med.* **3** 62–71
- Hynynen K, Damianou C and Jolesz F 1995 Mr monitoring of focused ultrasonic surgery of renal cortex: Experimental and simulation studies *J. Magn. Reson. Imaging* **5** 259
- Jia Z Q 1995 Temperature homogeneity and blood flow in renal hyperthermia *Master's Thesis* University of Toronto
- Kolios M C, Sherar M D and Hunt J W 1995 Large vessel cooling in heated tissues: a numerical study *Phys. Med. Biol.* **40** 477–94
- 1996 Blood flow cooling and ultrasonic lesion formation *Med. Phys.* **23** 1287–98
- Kolios M C, Sherar M D, Worthington A E and Hunt J W 1994 Modeling temperature gradients near large vessels in perfused tissues *Fundamentals of Biomedical Heat Transfer* HTD-vol 295, ed M A Ebadian and P H Oosthuizen (New York: American Society of Mechanical Engineers) pp 23–30
- Kolios M C, Worthington A E, Holdsworth D, Sherar M D and Hunt J W 1998 The investigation of large vessel effects on steady state and transient temperature distributions during tissue heating *Phys. Med. Biol.* submitted
- Kotte A, Van Leeuwen G, Debree J, Vanderkoijk J, Crezee H and Lagendijk J 1996 A description of discrete vessel segments in thermal modeling of tissues *Phys. Med. Biol.* **41** 865–84
- Lagendijk J J W 1990 Thermal models: principles and implementation *Introduction to the Clinical Aspects of Clinical Hyperthermia* ed S B Field and J W Hand (Bristol, PA: Taylor and Francis) pp 478–511
- Loyd D, Karlsson M, Erlandsson B E, Sjodin J G and Ask P 1997 Computer analysis of hyperthermia treatment of the prostate *Adv. Eng. Software* **28** 347–51
- Macfall J R, Prescott D M, Charles H C and Samulski T V 1996 H-1 MRI phase thermometry in-vivo in canine brain, muscle, and tumor-tissue *Med. Phys.* **23** 1775–82
- Malone E M and Wyman W R 1992 Interstitial laser photocoagulation of abdominal tumors *Adv. Gastrointest. Radiol.* **2** 221–41

- Martin G T, Haddad M G, Cravalho E G and Bowman H F 1992 Thermal model for the local microwave hyperthermia treatment of benign prostatic hyperplasia *IEEE Trans. Biomed. Eng.* **39** 836–44
- Mooibroek J and Langendijk J J W 1991 A fast and simple algorithm for the calculation of convective heat transfer by large vessels in three-dimensional inhomogeneous tissues *IEEE Trans. Biomed. Eng.* **38** 490–501
- Moros E G, Dutton A W, Roemer R B, Burton M and Hynynen K 1993 Experimental evaluation of two simple thermal models using hyperthermia *in vivo* *Int. J. Hyperth.* **9** 581–98
- Overgaard J, Gonzalez D G, Hulshof M, Arcangeli G, Dahl O and Mella S M and Bentzen O 1996 Hyperthermia as an adjuvant to radiation-therapy of recurrent or metastatic malignant-melanoma: a multicenter randomized trial by the European Society for Hyperthermic Oncology *Int. J. Hyperth.* **12** 13–20
- Pennes H H 1948 Analysis of tissue and arterial blood temperatures in the resting human forearm *J. Appl. Phys.* **1** 93–122
- Rawnsley R J, Roemer R B and Dutton A W 1994 The simulation of discrete vessel effects in experimental hyperthermia *J. Biomech. Eng.* **116** 256
- Roemer R B 1991 Optimal power deposition in hyperthermia I. The treatment goal: the ideal temperature distribution II. The role of large blood vessels *Int. J. Hyperth.* **7** 317–41
- Shaw A, Preston R C and Bacon D R 1996 Perfusion corrections for ultrasonic heating in nonperfused media *Ultrasound Med. Biol.* **22** 203–16
- ter Haar G 1995 Ultrasound focal beam surgery *Ultrasound Med. Biol.* **21** 1089–100
- Valdagni R and Amichetti M 1994 Report of long-term follow-up in a randomized trial comparing radiation therapy and radiation therapy plus hyperthermia to metastatic lymph nodes in stage IV head and neck patients *Int. J. Radiat. Oncol. Biol. Phys.* **28** 163–9
- Valvano J W, Sungwoo N and Anderson G T 1994 Analysis of the Weinbaum–Jiji model of blood flow in the canine kidney cortex for self-heated thermistors *J. Biomech. Eng.* **116** 201–7
- Vernon C C *et al* 1996 Radiotherapy with or without hyperthermia in the treatment of superficial localized breast-cancer: results from 5 randomized controlled trials *Int. J. Radiat. Oncol. Biol. Phys.* **35** 731–44
- Vitkin I A *et al* 1997 Magnetic resonance imaging of temperature changes during interstitial microwave heating: a phantom study *Med. Phys.* **24** 269–77
- Weinbaum S, Jiji L M and Lemons D E 1984 Theory and experiment for the effect of vascular microstructure on surface heat transfer-part I: Anatomical foundation and model conceptualization *J. Biomech. Eng.* **106** 321–30
- Weinbaum S, Xu L X, Zhu L and Ekpene A 1997 A new fundamental bioheat equation for muscle tissue. I. Blood perfusion term *J. Biomech. Eng.* **119** 278–88
- Whelan W M and Wyman D R 1995 Temperature reconstruction by estimating the thermophysical and optical properties of tissue during interstitial laser heating *Advances in Heat and Mass Transfer in Biotechnology* ed L J Hayes (New York: American Society of Mechanical Engineers) pp 17–26
- Wyman D R and Whelan W M 1994 Basic optothermal diffusion theory for interstitial laser photocoagulation *Med. Phys.* **21** 1651–6
- Zhu L, Lemons D E and Weinbaum S 1994 A new approach for predicting the enhancement in the effective conductivity of perfused tissue due to hyperthermia *Advances in Heat and Mass Transfer in Biological Systems* HTD-vol 288, ed L J Haynes and R B Roemer (New York: American Society of Mechanical Engineers) pp 37–43